

FUTURE COSMOLOGICAL CONSTRAINTS FROM FAST RADIO BURSTS

ANTHONY WALTERS,^{1,2} AMANDA WELTMAN,¹ B. M. GAENSLER,³ YIN-ZHE MA,^{2,4} AND AMADEUS WITZEMANN^{5,1}

¹*Department of Mathematics and Applied Mathematics, University of Cape Town, Cape Town, South Africa*

²*School of Chemistry and Physics, University of KwaZulu-Natal, Durban, 4000, South Africa*

³*Dunlap Institute for Astronomy and Astrophysics, University of Toronto, Toronto, ON M5S 3H4, Canada*

⁴*NAOC-UKZN Computational Astrophysics Centre (NUCAC), University of KwaZulu-Natal, Durban, 4000, South Africa*

⁵*Department of Physics and Astronomy, University of the Western Cape, Cape Town, South Africa*

Submitted to ApJ

ABSTRACT

We consider the possible observation of Fast Radio Bursts (FRBs) with planned future radio telescopes, and investigate how well the dispersions and redshifts of these signals might constrain cosmological parameters. We construct mock catalogues of FRB dispersion measure (DM) data and employ Markov Chain Monte Carlo (MCMC) analysis, with which we forecast and compare with existing constraints in the flat Λ CDM model, as well as some popular extensions that include dark energy equation of state and curvature parameters. We find that the scatter in DM observations caused by inhomogeneities in the intergalactic medium (IGM) poses a big challenge to the utility of FRBs as a cosmic probe. Only in the most optimistic case, with a high number of events and low IGM variance, do FRBs aid in improving current constraints. In particular, when FRBs are combined with CMB+BAO+SNe+ H_0 data, we find the biggest improvement comes in the $\Omega_b h^2$ constraint. Also, we find that the dark energy equation of state is poorly constrained, while the constraint on the curvature parameter Ω_k , shows some improvement when combined with current constraints. When FRBs are combined with future BAO data from 21cm Intensity Mapping (IM), we find little improvement over the constraints from BAOs alone. However, the inclusion of FRBs introduces an additional parameter constraint, $\Omega_b h^2$, which turns out to be comparable to existing constraints. This suggests that FRBs provide valuable information about the cosmological baryon density in the intermediate redshift Universe, independent of high redshift CMB data.

Keywords: cosmological parameters, cosmology: theory, dark energy — radio continuum: general

1. INTRODUCTION

Improvements in cosmological measurement in recent years have been said to hail an era of “precision cosmology”, with observations of the cosmic microwave background (CMB) temperature anisotropies (Hinshaw et al. 2013; Planck Collaboration et al. 2016a,b), baryon acoustic oscillation (BAO) wiggles in the galaxy power spectrum (Beutler et al. 2011; Anderson et al. 2014; Ross et al. 2015), luminosity distance-redshift relation of Type Ia supernovae (SNIa) (Riess et al. 2004, 2007; Kowalski et al. 2008; Betoule et al. 2014), local distance ladder (Riess et al. 2016), galaxy clustering and weak lensing (DES Collaboration et al. 2017), and direct detection of gravitational waves (Abbott et al. 2017), providing constraints on cosmological model parameters at percent, or sub-percent, level precision. Since the discovery of the accelerated expansion of the Universe, these observations have cemented the emergence of the flat Λ CDM model as the standard model of cosmology, in which global spatial curvature is zero, and the energy budget of the Universe is dominated by “dark energy” in the form of a cosmological constant, Λ . However, beyond the Λ CDM paradigm there are a large number of dark energy models aimed at explaining the accelerated expansion of the Universe (see reviews (Li et al. 2011; Joyce et al. 2015), and references therein), and so understanding the nature of dark energy remains one of the central pursuits in modern cosmology. To this end, it has become common observational practice to constrain the dark energy equation of state, $w(z)$, and check for deviations from the Λ CDM value of $w = \text{const.} = -1$. While observational probes do not indicate any significant departure from Λ CDM (Huterer & Shafer 2017), there is still room to tighten constraints and thereby rule out competing alternatives for dark energy. In particular, by tuning the parameters of alternative theories of dark energy, one can recover the behaviour of Λ CDM model at both the background expansion and perturbation levels (Li et al. 2011; Joyce et al. 2015).

Observations of the CMB together with SNIa and BAO constrain the spatial curvature parameter to be very small, $|\Omega_k| < 0.005$ (Planck Collaboration et al. 2016a), consistent with the flat Λ CDM model, and the inflationary picture of the early Universe. However, model independent constraints from low redshift probes are not nearly as strong, with SNIa alone preferring an open universe with $\Omega_k \sim 0.2$ (Räsänen et al. 2015). Similarly, constraints on the baryon fraction, Ω_b , derived from observations of the CMB, and the abundance of light elements together with the theory of Big Bang Nucleosynthesis (BBN) (Cooke et al. 2016), are both rooted in high redshift physics. And while these constraints are

somewhat consistent, the BBN results strongly depend on nuclear cross section data (Cooke et al. 2016; Dvorkin et al. 2016). Thus, independent and precise low redshift probes of spatial curvature and the baryon density parameter which confirm the constraints from high redshift data are of observational and theoretical interest.

Recently, a promising new astrophysical phenomenon, so called Fast Radio Bursts (FRBs) (Lorimer et al. 2007; Keane et al. 2011; Thornton et al. 2013; Spitler et al. 2014; Petroff et al. 2015; Burke-Spolaor & Bannister 2014; Ravi et al. 2015; Champion et al. 2016; Masui et al. 2015; Keane et al. 2016; Ravi et al. 2016; Caleb et al. 2017; Petroff et al. 2017), has emerged. An FRB is characterised by a brief pulse in the radio spectrum with a large dispersion in the arrival time of its frequency components, consistent with the propagation of an electromagnetic wave through a cold plasma. To date a total of 25 such FRBs ¹ have been detected, primarily by the the Parkes Telescope in Australia, but more recently interferometric detections have also been reported. Considering the greatly improved sensitivity of upcoming radio telescopes, expectations are high that many more FRB events will be observed in the near future (Rajwade & Lorimer 2017; Fialkov & Loeb 2017). While their exact location and formation mechanism is still a subject of ongoing research (Kashiyama et al. 2013; Totani 2013; Zhang 2014; Fuller & Ott 2015; Lyubarsky 2014; Cordes & Wasserman 2016; Ghisellini 2017; Gu et al. 2016; Wang et al. 2016; Beloborodov 2017; Locatelli & Ghibellini 2017; Kumar et al. 2017; Katz 2017; Ghisellini & Locatelli 2017; Thompson 2017), their excessively large dispersion measures (DMs) argue that they have an extragalactic origin (Xu & Han 2015). Indeed, one FRB event has been sufficiently localised to be associated with a host galaxy at $z = 0.19$ (Tendulkar et al. 2017). Should one be able to associate a redshift with enough FRBs, it would give access to the $\text{DM}(z)$ relation, which may provide a new probe of the cosmos (Deng & Zhang 2014; Zhou et al. 2014; Gao et al. 2014; Yang & Zhang 2016), possibly complementary to existing techniques. In this paper we assess the potential for using FRB observations to constrain the parameter space of various cosmological models, and whether this may improve the existing constraints coming from other observations.

The outline of this paper is as follows: The details of modelling an extragalactic population of FRBs, constructing a mock catalogue of DM observations, and extracting and combining cosmological parameter con-

¹ From version 2.0 of the FRB catalogue (Petroff et al. 2016) found at <http://www.frbcat.org/>, accessed on 17 November 2017

straints is given in §2. Parameter constraint forecasts from the mock FRB data, and its combination with CMB + BAO + SNIa + H_0 (hereafter referred to as CBSH), is given in §3.1 for the flat Λ CDM model, and in §3.2 for 1- and 2-parameter extensions to the flat Λ CDM model. Possible synergies with other experiments are discussed in §4.

2. COSMOLOGY WITH FAST RADIO BURSTS

2.1. Dispersion of the Intergalactic Medium

The DM of an FRB is associated with the propagation of a radio wave through a cold plasma, and is related to the path length from the emission event to observation, and the distribution of free electrons along that path, $DM = \int n_e dl$. If FRBs are of extragalactic origin their observed dispersion measure, DM_{obs} , should be the sum of a number of different contributions, namely; from propagating through its host galaxy, DM_{HG} , the intergalactic medium (IGM), DM_{IGM} , and the Milky Way, DM_{MW} (Deng & Zhang 2014). Since DM_{MW} as a function of Galactic latitude is well known from pulsar observations (Yao et al. 2017), and its contribution to DM_{obs} is relatively small in most cases, we assume it can be reliably subtracted. We choose to work with the extragalactic dispersion measure, given by (Yang & Zhang 2016)

$$DM_E \equiv DM_{\text{obs}} - DM_{\text{MW}} = DM_{\text{IGM}} + DM_{\text{HG}}, \quad (1)$$

where DM_{HG} is defined in the observers frame, and related to that at the emission event by

$$DM_{\text{HG}} = \frac{DM_{\text{HG,loc}}}{1+z}. \quad (2)$$

This contribution is not well known and is expected to depend on the type of host galaxy, its inclination relative to the observer, and the location of the FRB inside the host galaxy (Xu & Han 2015; Yang & Zhang 2016), and so we include this as a source of uncertainty in our analysis.

The intergalactic medium is inhomogeneous and so $DM_{\text{IGM}}(z)$ will have a large sightline-to-sightline variance, with estimates ranging between ~ 200 and 400 pc cm^{-3} by $z \sim 1.5$ (McQuinn 2014). It has however been shown that with enough FRB events in small enough redshift bins, the mean dispersion measure in each bin will approach the Friedmann-Lemaître-Robertson-Walker (FLRW) background value to good approximation. Specifically, with $N \sim 80$ events in the redshift bin $1 \leq z \leq 1.05$, the mean dispersion measure will be with 5% of the FLRW background value, at 95.4% confidence (Zhou et al. 2014). This is essential if one wishes to measure the cosmological parameters with any precision.

Assuming a non-flat FLRW Universe that is dominated by matter and dark energy, one finds the average (background) dispersion measure of the intergalactic medium is (Deng & Zhang 2014; Zhou et al. 2014; Gao et al. 2014)

$$\langle DM_{\text{IGM}}(z) \rangle = \frac{3cH_0\Omega_b f_{\text{IGM}}}{8\pi Gm_p} \int_0^z \frac{\chi(z')(1+z')}{E(z')} dz', \quad (3)$$

where

$$E(z) = [(1+z)^3\Omega_m + f(z)\Omega_{\text{DE}} + (1+z)^2\Omega_k]^{1/2}, \quad (4)$$

$$\chi(z) = Y_H\chi_{e,H}(z) + \frac{1}{2}Y_p\chi_{e,He}(z), \quad (5)$$

$$f(z) = \exp \left[3 \int_0^z \frac{(1+w(z''))dz''}{(1+z'')} \right], \quad (6)$$

and H_0 is the value of the Hubble parameter today, Ω_b is the baryon mass fraction of the Universe, f_{IGM} is the fraction of baryon mass in the intergalactic medium, $Y_H = 3/4$ ($Y_p = 1/4$) is the hydrogen (helium) mass fraction in the intergalactic medium, and $\chi_{e,H}$ ($\chi_{e,He}$) is the ionisation fraction of hydrogen (helium). The cosmological density parameters for matter and curvature are Ω_m and Ω_k , respectively, and the dark energy density parameter is given by the constraint $\Omega_{\text{DE}} \equiv 1 - \Omega_m - \Omega_k$.

We allow for the equation of state of dark energy, w , to vary with time, and parameterise it by (Chevallier & Polarski 2001; Linder 2003)

$$w(z) = w_0 + w_a \frac{z}{1+z}, \quad (7)$$

where w_0 and w_a are the CPL parameters. Substituting (7) into (6), and integrating, gives an exact analytic expression for the growth of dark energy density as a function of redshift

$$f(z) = (1+z)^{3(1+w_0+w_a)} \exp \left[-3w_a \frac{z}{1+z} \right]. \quad (8)$$

Choosing $(w_0, w_a) = (-1, 0)$ in (6) gives $f(z) = \text{const.}$, corresponding to the Λ CDM model, in which dark energy is a cosmological constant.

For simplicity (to avoid modelling any astrophysics) we restrict our analysis to the region $z \leq 3$, since current observations suggest that both hydrogen and helium are fully ionised there (Meiksin 2009; Becker et al. 2011), and thus we can safely take $\chi_{e,H} = \chi_{e,He} = 1$ in (5). This gives a constant $\chi(z) = 7/8$ in the region of interest. The f_{IGM} term presents some complications. Strictly speaking, f_{IGM} is a function of redshift ($f_{\text{IGM}} = f_{\text{IGM}}(z)$) ranging from about 0.9 at $z \gtrsim 1.5$ to 0.82 at $z \leq 0.4$ (Meiksin 2009; Shull et al. 2012), and should be included inside the integral in (3). As a first approximation we neglect the effect of evolving f_{IGM} , and set it to a constant.

2.2. Telescope Time and the Mock Catalogue

Based on current detections, the FRB event rate in the Universe is expected to be high, and given the improved design sensitivity of future radio telescopes, their detection rate is expected to increase significantly. This value, of course, will depend on the exact specifications of the telescope, and the true distribution and spectral profile of FRBs. For example, assuming they live only in low mass host galaxies, and have a Gaussian-like spectral profile, the mid-frequency component of the Square Kilometre Array (SKA) is expected to detect FRBs out to $z \sim 3.2$ at a rate of $\sim 10^3 \text{ sky}^{-1} \text{ day}^{-1}$ (Fialkov & Loeb 2017). In the more immediate future, the Hydrogen Intensity Real-time Analysis eXperiment (HIRAX) (Newburgh et al. 2016) and the Canadian Hydrogen Intensity Mapping Experiment (CHIME) (Bandura et al. 2014), are expected to detect $\sim 50 - 100 \text{ day}^{-1}$ and $\sim 30 - 100 \text{ day}^{-1}$, respectively (Rajwade & Lorimer 2017). Assuming that 5% of the detected FRBs can be sufficiently localised to be associated with a host galaxy, the rate of detection and localisation would be roughly $\sim 2 - 5 \text{ day}^{-1}$ for HIRAX and CHIME, and far higher for the SKA. This suggests that a large catalogue of localised FRBs could be built up relatively quickly, and the main bottleneck in obtaining a catalogue of $DM(z)$ data will be acquiring the redshifts. Given the bright emission lines in the spectrum of the host galaxy for the repeating FRB 121102 (Tendulkar et al. 2017), a mid-to large-sized optical telescope should be able to obtain ~ 10 redshifts for FRB host galaxies per night; we thus estimate that a redshift catalogue with $N_{\text{FRB}} = 1000$ will take approximately 100 nights of observing to construct, which would be feasible with a dedicated observing program spread over a few years.

Motivated by a phenomenological model for the distribution of gamma ray bursts, we assume the redshift distribution of FRBs is given by $P(z) = ze^{-z}$ (Zhou et al. 2014; Yang & Zhang 2016), and simulate $DM_E(z)$ measurements, given by the far right side of (1). For this we assume a flat Λ CDM background as the fiducial cosmology, and use the best fit CBSH parameter values provided by the Planck 2015 data release², listed in the second column of table 2. We also take $f_{\text{IGM}} = 0.83$ (Shull et al. 2012). We assume the value for DM_{IGM} is given by (3) and assume a scatter about the line (due to matter inhomogeneities in IGM) follows a normal distribution. We also assume a mean value for the contribution from the host galaxy, $\langle DM_{\text{HG,loc}} \rangle$, and normally

distributed scatter with standard deviation $\sigma_{\text{HG,loc}}$, and thus model the mock FRB catalogue using

$$DM_E(z) = \mathcal{N}(\langle DM_{\text{IGM}}(z) \rangle, \sigma_{\text{IGM}}) + \frac{\mathcal{N}(\langle DM_{\text{HG,loc}} \rangle, \sigma_{\text{HG,loc}})}{1 + z}. \quad (9)$$

The value of $DM_{\text{HG,loc}}$ is expected to contain contributions from the Interstellar Medium (ISM) of the FRB host galaxy and near-source plasma. Since FRB progenitors and their emission mechanisms are as yet unknown, reasonable values of $\langle DM_{\text{HG,loc}} \rangle$ and $\sigma_{\text{HG,loc}}$ are still debatable. Here we assume nothing about the host galaxy type or location of the FRB therein, just that there is a significant contribution to $DM_{\text{HG,loc}}$ due to near source-plasma, and thus take $\langle DM_{\text{HG,loc}} \rangle = 200 \text{ pc cm}^{-3}$ and $\sigma_{\text{HG,loc}} = 50 \text{ pc cm}^{-3}$ (Yang & Zhang 2016). To investigate the effect of sample size and IGM inhomogeneities on resulting constraints, we construct a number of mock catalogues with various values for σ_{IGM} and N_{FRB} . For the most optimistic sample, we choose $(N_{\text{FRB}}, \sigma_{\text{IGM}}) = (1000, 200)$. See table 1 for a summary of the various catalogues.

	N_{FRB}	$\sigma_{\text{IGM}} [\text{pc cm}^{-3}]$	z_{lim}
FRB1	1000	200	3
FRB2	1000	400	3
FRB3	100	200	3

Table 1. Parameter values used when populating the various mock FRB catalogues. The number of FRB events is shown in the first column, the sightline-to-sightline variance in the second column, and the limiting redshift in the third column.

2.3. Parameter Estimation and Priors

For the MCMC analysis we use the χ^2 statistic as a measure of likelihood for the parameter values. The log-likelihood function is given by

$$\ln \mathcal{L}_{\text{FRB}}(\theta|d) = -\frac{1}{2} \sum_i \frac{(DM_{E,i} - \langle DM_E \rangle)^2}{\sigma_{\text{IGM},i}^2 + [\sigma_{\text{HG,loc},i}/(1 + z_i)]^2}, \quad (10)$$

where θ is the set of fitting parameters, d is the FRB data, and the sum over i represents the sequence of FRB data in the sample. Constraints on the flat Λ CDM model parameters are obtained by setting $\Omega_k = 0$ in (3) and $w = -1$ in (6), and then fitting the mock data for $\theta = (\Omega_m, H_0, \Omega_b h^2, \langle DM_{\text{HG,loc}} \rangle)$. To investigate spatial curvature in the Λ CDM model, we allow

² Planck 2015 covariance matrices and MCMC chains can be found at <http://pla.esac.esa.int/pla/#cosmology>

for $\Omega_k \neq 0$ in (3), and include it as an additional fitting parameter. For the dark energy constraints we consider two model parametrisations with flat spatial geometry. In the first case, we extend to the w CDM model, allowing for $w = \text{const.} \neq -1$. We set $\Omega_k = 0$ in (3) and $(w_0, w_a) = (w, 0)$ in (7), and fit the data for $\theta = (w, \Omega_m, H_0, \Omega_b h^2, \langle \text{DM}_{\text{HG,loc}} \rangle)$. In the second case, we allow for dark energy to vary with time and use the CPL parametrisation (7), and thus set $\Omega_k = 0$ in (3), and fit the FRB data for the parameters $\theta = (w_0, w_a, \Omega_m, H_0, \Omega_b h^2, \langle \text{DM}_{\text{HG,loc}} \rangle)$. For all the extended models, we fit to the flat Λ CDM data described in §2.2, and examine how close to fiducial values the additional parameters are constrained. This also allows us to easily combine the constraints with existing data, which is consistent with flat Λ CDM.

We use the Python package *emcee* (Foreman-Mackey et al. 2013) to determine the posterior distribution for the parameters, and *GetDist*³ for plotting and analysis. When prior information is included in the analysis we use the respective covariance matrix provided by the Planck 2015 data release. We thus calculate the priors according to

$$\ln P(\theta) = -\frac{1}{2} \xi \mathbf{C}^{-1} \xi, \quad (11)$$

where $P(\theta)$ is the prior probability associated with the parameter values θ , \mathbf{C} is a (square) covariance matrix, and $\xi = \theta - \theta_{\text{fiducial}}$ is the displacement in parameters space between the relevant parameter values and the fiducial values. To avoid rescaling the CBSH covariance matrix to accommodate for Ω_b , we set up our code to fit for $\Omega_b h^2$, which is a primary parameter in the Planck analysis, and thus its covariance is provided.

3. PARAMETER CONSTRAINTS FORECAST

Here we discuss the FRB constraints forecast for the flat Λ CDM model and some simple 1- and 2-parameter extensions. In all models, when fitting the most optimistic catalogue, FRB1, we find that H_0 and $\Omega_b h^2$ are unconstrained when no prior information about the parameters is included. This is unsurprising, since $\text{DM}_{\text{IGM}} \propto \Omega_b H_0$. And as a result, the other cosmological parameters are only very weakly constrained, if at all. In all models we find the measurement precision of Ω_m is tens of a percent, hardly good enough to be considered a tool for ‘precision cosmology’ at the sub-percent level. We thus include the CBSH covariance matrix in our analysis in order to determine if FRBs offer any additional constraining power.

In figure 1 we plot a compilation of the marginalised 1D posterior probability distributions for the cosmological parameters, obtained from a combination of CBSH constraints and the various mock FRB catalogues listed in Table 1. Black lines indicate the CBSH constraints used in the covariance matrix for calculating the priors, given by Eq. (11). The solid red, dot-dashed blue and dotted green lines indicate the constraints when CBSH is combined with the FRB1, FRB2 and FRB3 catalogues, respectively. The corresponding $2\text{-}\sigma$ confidence intervals are listed in table 2. We deal with the various cosmological models in turn, below.

3.1. Flat Λ CDM

Including the CBSH covariance matrix gives the combined constraints, CBSH+FRB, shown in the top row of figure 1. We find that the posteriors for H_0 and Ω_m show only a minor improvement over their priors, as can be seen in the second and third column. The most improved constraint is given by $\Omega_b h^2 = 0.02235^{+0.00021}_{-0.00021}$, which corresponds to a $\sim 20\%$ reduction in the size of the $2\text{-}\sigma$ confidence interval of the CBSH prior. The source of this improvement can be seen in figure 2, where we plot constraints in the $\Omega_m\text{-}\Omega_b h^2$ plane. Here we include the CBSH prior for H_0 with the FRB1 analysis, and plot the resulting constraint (grey) with the CBSH constraints (red). The degeneracy directions of the two eclipses are different, and their intersection gives the combined constrain (blue). Thus, given our current knowledge of the Λ CDM parameters and their covariance, DM observations will provide more information on $\Omega_b h^2$ than the other cosmological parameters.

Constraints derived from a combination of CBSH with the various FRB catalogues, represented by the coloured curves in the top row of figure 1, illustrate the effect of varying the IGM inhomogeneity and sample size. Increasing the IGM inhomogeneity from $\sigma_{\text{IGM}} = 200 \text{ pccm}^{-3}$ to $\sigma_{\text{IGM}} = 400 \text{ pccm}^{-3}$ weakens the constraints considerably. The strongest constraint in this case becomes $\Omega_b h^2 = 0.02227^{+0.00025}_{-0.00025}$, which corresponds to a $\sim 5\%$ reduction in size of the $2\text{-}\sigma$ interval of the CBSH constraint. Similarly, reducing the samples size to $N_{\text{FRB}} = 100$, and keeping IGM inhomogeneity low at $\sigma_{\text{IGM}} = 200 \text{ pccm}^{-3}$ also weakens any improvement offered by FRBs. In this case we find $\Omega_b h^2 = 0.02224^{+0.00026}_{-0.00026}$, which is a $\sim 2\%$ reduction in the size of the CBSH $2\text{-}\sigma$ interval. Clearly one needs many FRB events in order to mitigate the effects of IGM inhomogeneity.

3.2. Extensions Beyond Flat Λ CDM

Curvature—When no priors are included, we find that Ω_k is unconstrained by FRB observations alone. Even

³ Packages available at <https://github.com/cmbant/getdist>

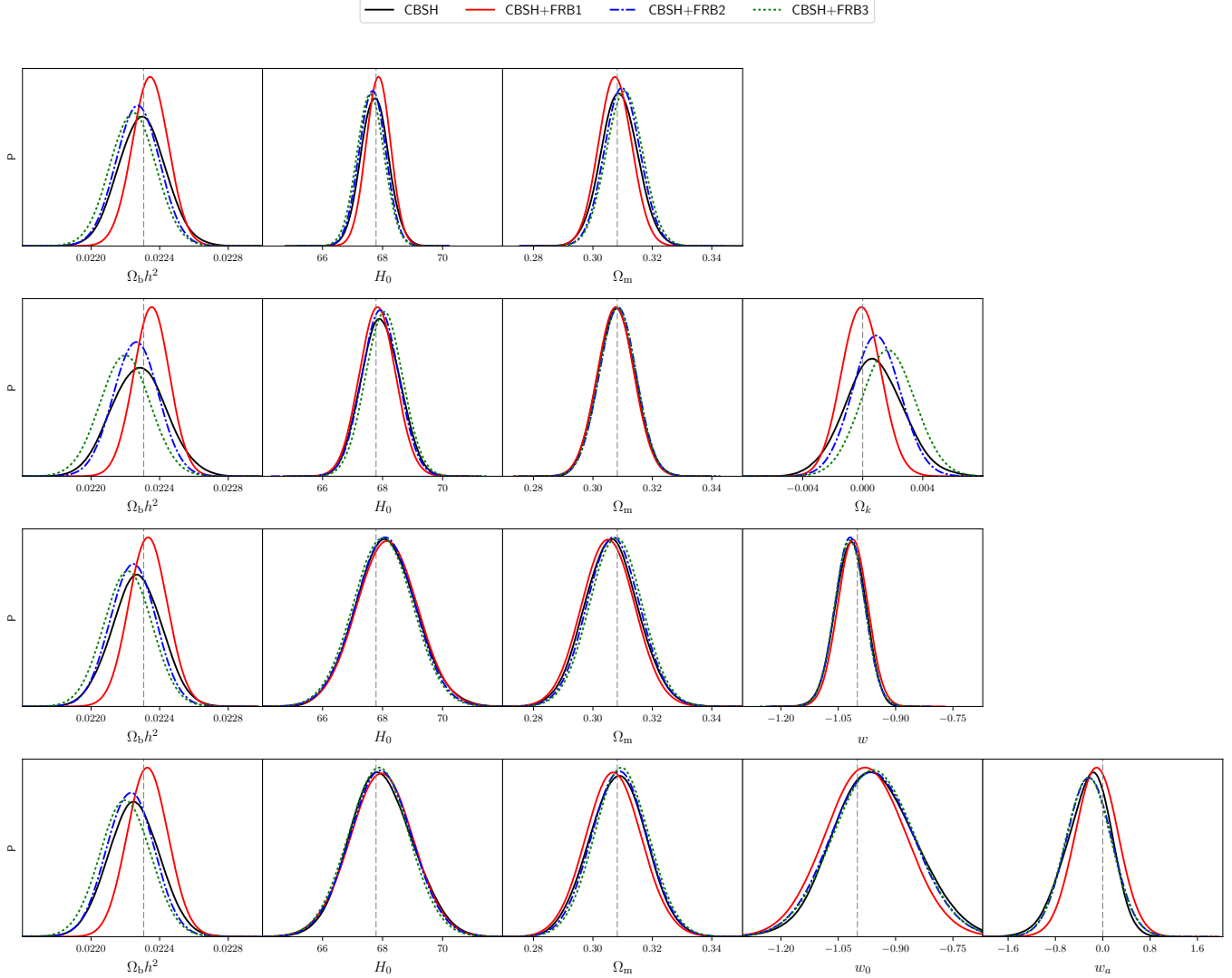


Figure 1. Marginalised posterior probability distributions obtained from a combination of CBSH constraints and the various mock FRB catalogues listed in Table 1, for all cosmological model parametrisations considered here. From the top to bottom row we list constraints for flat Λ CDM, Λ CDM with spatial curvature, flat w CDM, and flat w_0w_a CDM. Black lines indicate the CBSH constraints used as priors. The red, blue and green lines indicate the constraints when CBSH is combined with the FRB1, FRB2 and FRB3 catalogues, respectively. Dashed grey lines indicates the true parameter values used in the mock FRB catalogues (corresponding to the CBSH best fit parameter values in the flat Λ CDM model). The area under all curves has been normalised to unity.

when the CBSH covariance matrix for $(\Omega_m, H_0, \Omega_b h^2)$ is included, the constraint on Ω_k remains very weak. However, with the full CBSH covariance matrix included we find $\Omega_k = -0.0001^{+0.0026}_{-0.0026}$ and $\Omega_b h^2 = 0.02235^{+0.00020}_{-0.00021}$. This corresponds to a $\sim 35\%$ reduction in the size of the CBSH $2\text{-}\sigma$ intervals for $\Omega_b h^2$ and Ω_k . The source of this improvement is illustrated in figure 3 where we plot the 2D marginalised constraints in the $\Omega_b h^2$ - Ω_k plane. The FRB1 constraints with CBSH covariance for $(\Omega_m, H_0, \Omega_b h^2)$ are shown in grey, and the CBSH constraints in red. It is clear that the grey contour very weakly constrains Ω_k . However, it runs orthogonal to

the CBSH constraint, and intersects it in a way that simultaneously improves both the Ω_k and $\Omega_b h^2$ constraints when the data are combined, shown in blue. Posteriors for Ω_m and H_0 are dominated by their priors, as can be seen in the second row of figure 1.

Increasing the IGM variance to $\sigma_{\text{IGM}} = 400 \text{ pc cm}^{-3}$ degrades the constraints to $\Omega_b h^2 = 0.02226^{+0.00026}_{-0.00026}$ and $\Omega_k = 0.0009^{+0.0032}_{-0.0032}$, which corresponds to a $\sim 18\%$ reduction in the size of CBSH $2\text{-}\sigma$ interval. Similarly, reducing the sample size to $N_{\text{FRB}} = 100$, we find $\Omega_b h^2 = 0.02220^{+0.00029}_{-0.00029}$ and $\Omega_k = 0.0017^{+0.0035}_{-0.0035}$, which corresponds to a $\sim 10\%$ reduction in the size of the CBSH $2\text{-}\sigma$

Parameter	95% limits			
	CBSH	CBSH+FRB1	CBSH+FRB2	CBSH+FRB3
$10^3 \Omega_m$	$3.09^{+0.12}_{-0.12}$	$3.07^{+0.11}_{-0.11}$	$3.10^{+0.12}_{-0.12}$	$3.11^{+0.12}_{-0.12}$
H_0	$67.74^{+0.92}_{-0.90}$	$67.86^{+0.79}_{-0.80}$	$67.66^{+0.86}_{-0.87}$	$67.60^{+0.89}_{-0.89}$
$10^2 \Omega_b h^2$	$2.230^{+0.027}_{-0.026}$	$2.235^{+0.021}_{-0.021}$	$2.227^{+0.025}_{-0.025}$	$2.224^{+0.026}_{-0.026}$
$\langle DM_{\text{HG,loc}} \rangle$		215^{+30}_{-30}	189^{+60}_{-60}	161^{+90}_{-90}
$10^3 \Omega_k$	$0.8^{+4.0}_{-3.9}$	$-0.1^{+2.6}_{-2.6}$	$0.9^{+3.2}_{-3.2}$	$1.7^{+3.5}_{-3.5}$
$10 \Omega_m$	$3.08^{+0.12}_{-0.12}$	$3.08^{+0.12}_{-0.12}$	$3.08^{+0.12}_{-0.12}$	$3.08^{+0.12}_{-0.12}$
H_0	$67.9^{+1.3}_{-1.2}$	$67.8^{+1.2}_{-1.2}$	$67.9^{+1.2}_{-1.2}$	$68.0^{+1.2}_{-1.2}$
$10^2 \Omega_b h^2$	$2.228^{+0.032}_{-0.031}$	$2.235^{+0.020}_{-0.021}$	$2.226^{+0.026}_{-0.026}$	$2.220^{+0.029}_{-0.029}$
$\langle DM_{\text{HG,loc}} \rangle$		201^{+40}_{-40}	196^{+60}_{-60}	177^{+90}_{-90}
w	$-1.019^{+0.075}_{-0.080}$	$-1.012^{+0.077}_{-0.078}$	$-1.020^{+0.077}_{-0.077}$	$-1.020^{+0.077}_{-0.077}$
$10 \Omega_m$	$3.06^{+0.18}_{-0.18}$	$3.05^{+0.18}_{-0.17}$	$3.07^{+0.17}_{-0.17}$	$3.08^{+0.17}_{-0.17}$
H_0	$68.1^{+2.1}_{-1.9}$	$68.1^{+2.0}_{-2.0}$	$68.1^{+1.9}_{-1.9}$	$68.0^{+1.9}_{-1.9}$
$10^2 \Omega_b h^2$	$2.227^{+0.027}_{-0.029}$	$2.233^{+0.022}_{-0.022}$	$2.224^{+0.026}_{-0.026}$	$2.221^{+0.028}_{-0.028}$
$\langle DM_{\text{HG,loc}} \rangle$		204^{+30}_{-30}	191^{+60}_{-60}	163^{+90}_{-90}
w_0	$-0.95^{+0.21}_{-0.20}$	$-0.98^{+0.21}_{-0.21}$	$-0.96^{+0.21}_{-0.21}$	$-0.96^{+0.21}_{-0.21}$
w_a	$-0.25^{+0.72}_{-0.78}$	$-0.10^{+0.71}_{-0.71}$	$-0.23^{+0.76}_{-0.76}$	$-0.24^{+0.77}_{-0.76}$
$10 \Omega_m$	$3.08^{+0.19}_{-0.19}$	$3.07^{+0.19}_{-0.18}$	$3.09^{+0.18}_{-0.18}$	$3.10^{+0.18}_{-0.18}$
H_0	$68.0^{+2.0}_{-2.0}$	$68.0^{+2.0}_{-2.1}$	$67.9^{+2.0}_{-2.0}$	$67.9^{+2.0}_{-2.0}$
$10^2 \Omega_b h^2$	$2.225^{+0.030}_{-0.029}$	$2.233^{+0.024}_{-0.023}$	$2.223^{+0.027}_{-0.027}$	$2.220^{+0.029}_{-0.029}$
$\langle DM_{\text{HG,loc}} \rangle$		205^{+30}_{-30}	195^{+60}_{-60}	167^{+90}_{-90}

Table 2. Parameter constraints for flat Λ CDM and some 1- and 2-parameter extensions, namely; Λ CDM with spatial curvature, w CDM and $w_0 w_a$ CDM. The first column lists the constraints, for each model, obtained from the FRB1 catalogue alone, the second column lists the corresponding CBSH constraints, and the third fourth and fifth columns list the combined constraints from the various catalogues listed in Table 1.

σ intervals. Thus, while FRB observations alone do not constrain Ω_k , they add some constraining power when current parameter covariance is included. As in the flat Λ CDM case, many FRBs are needed to realise this improvement.

Testing Concordance—When the CBSH covariance for $(H_0, \Omega_b h^2)$ is included in the analysis, the resulting 2D marginalised constraint contours are, in all cases, larger than the CBSH ones. A crucial difference between this result and that of (Zhou et al. 2014; Gao et al. 2014), is that the previous authors assumed perfect knowledge of H_0 and Ω_b , and neglected any contribution from the host galaxy, and thus got a very narrow FRB contour in the w - Ω_m plane, which they showed would intersect with, and improve, the current constraints. Alas, we find this is not the case if realistic prior knowledge about H_0 and $\Omega_b h^2$ is included.

In the third row of figure 1 we plot the normalised 1D posterior distributions for the w CDM model param-

eters. For all catalogues listed in table 1 we find that the posteriors are dominated by their priors, with the exception being $\Omega_b h^2$. When using the most optimistic catalogue, we find $\Omega_b h^2 = 0.02233^{+0.00022}_{-0.00022}$, which corresponds to a $\sim 20\%$ reduction in the size of the $2\text{-}\sigma$ confidence interval of the CBSH prior. Increasing the IGM variance to $\sigma_{\text{IGM}} = 400 \text{ pc cm}^{-3}$ weakens this improvement to a few percent. There is no improvement in the $\Omega_b h^2$ constraint if the sample size is reduced to $N_{\text{FRB}} = 100$.

Dynamical Dark Energy—The normalised 1D posterior distributions can be seen in the bottom row of figure 1. With the CBSH covariance included in the FRB1 analysis, we find that all posteriors are dominated by the CBSH priors, with the exception being $\Omega_b h^2 = 0.02233^{+0.00024}_{-0.00023}$, which corresponds to a $\sim 20\%$ reduction in the size of the CBSH $2\text{-}\sigma$ interval. As in the w CDM model, increasing the IGM variance to $\sigma_{\text{IGM}} = 400 \text{ pc cm}^{-3}$ weakens this improvement to a

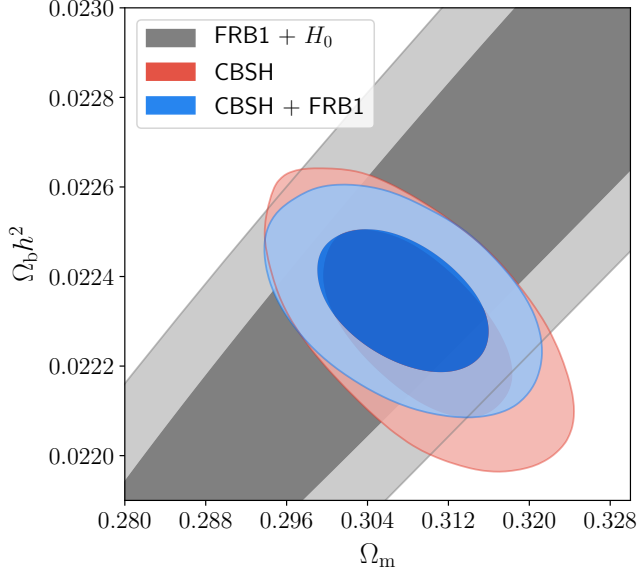


Figure 2. Flat Λ CDM parameter constraints in the Ω_m - $\Omega_b h^2$ plane. Constraints obtained from the FRB1 catalogue with a CBSH prior on H_0 are shown in grey, the CBSH constraints are shown in red, and the combined constraints are shown in blue. Without including priors, the FRB constraints are very weak, and so have been omitted from this plot.

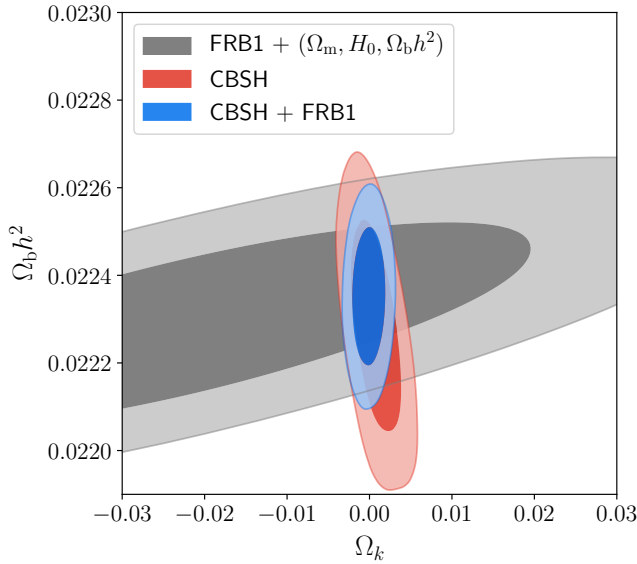


Figure 3. Non-Flat Λ CDM marginalised 2-D posterior distribution in the $\Omega_b h^2$ - Ω_k plane. FRB constraints, when including CBSH covariance for $(\Omega_m, H_0, \Omega_b h^2)$, are shown in grey, CBSH constraints are shown in red, and the combined constraints are shown in blue. Without including priors, the FRB constraints are very weak, and so have been omitted from this plot.

few percent, and there is no improvement if the sample

size is reduced to $N_{\text{FRB}} = 100$. Thus, even under our most optimistic assumptions, we find FRB provide no additional information about the nature of dark energy.

4. SYNERGY WITH 21CM BAO EXPERIMENTS

Future 21cm Intensity Mapping (IM) experiments designed to measure BAO in the distribution of neutral hydrogen, such as HIRAX and CHIME, are expected to measure numerous FRBs during the course of their observing runs. Since these FRB detections will essentially come for free (although the redshift will require dedicated observations), we aim determine whether their inclusion in the data analysis might improve the constraint forecasts for the 21cm IM BAO alone. Here we perform a simultaneous MCMC analysis of the FRB1 catalogue with the mock 21cm IM BAO measurement presented in (Witzemann et al. 2017). The mock BAO data is generated for HIRAX, which is a near-future radio interferometer planned to be built in South Africa. It will consist of 1024 6m dishes, covering the frequency range 400-800 MHz, corresponding to a redshifts between 0.8 and 2.5. We assume an integration time of 1 year, and a non-linear cutoff scale at $z = 0$ of $k_{\text{NL},0} = 0.2 \text{ Mpc}^{-1}$, which evolves with redshift according to the results from (Smith et al. 2003), $k_{\text{max}} = k_{\text{NL},0}(1+z)^{2/(2+n_s)}$ with the spectral index n_s . We use these specifications and a slightly adapted version of the publicly available code from (Bull et al. 2015) to calculate covariance matrices \mathbf{C}_{BAO} for the Hubble rate, H , and angular diameter distance, D_A , in $N = 20$ equally spaced frequency bins. We consider correlations between H and D_A and assume different bins to be uncorrelated. For the MCMC analysis, the likelihood of a given set of cosmological parameters is then calculated using these measurements together with the FRB1 catalogue, according to

$$\ln \mathcal{L} = \ln \mathcal{L}_{\text{BAO}} + \ln \mathcal{L}_{\text{FRB}}, \quad (12)$$

where

$$\ln \mathcal{L}_{\text{BAO}} = -\frac{1}{2} \sum_{j=1}^N (\nu_j - \mu_j)^T \mathbf{C}_{\text{BAO}}^{-1}(z_j) (\nu_j - \mu_j) \quad (13)$$

and $\ln \mathcal{L}_{\text{FRB}}$ is given by (10). Further definitions used are $\nu_j = (D_A(z_j, \theta), H(z_j, \theta))$ as well as $\mu_j = (D_A(z_j, \theta_{\text{fid}}), H(z_j, \theta_{\text{fid}}))$. All priors are flat and identical to the ones used in the FRB analysis.

We find that FRBs add little to the constraints coming from 21cm BAO alone — they only tend to remove some of the non-Gaussian tails in the BAO posteriors. However, they do add an additional parameter into the fitting process, $\Omega_b h^2$, which turns out to be the most competitive constraint. We find $\Omega_b h^2 = 0.02235^{+0.00032}_{-0.00032}$,

which is comparable to the current CBSH constraint, and entirely independent. This suggests that, when combined with 21cm IM BAO measurements, FRBs may provide an intermediate redshift measure of the cosmological baryon density, independent of high redshift CMB constraints.

5. CONCLUSIONS

In this paper we have investigated how future observations of FRBs might help to constrain cosmological parameters. By constructing various mock catalogues of FRB observations, and using MCMC techniques, we have forecast constraints for parameters in the flat Λ CDM model, as well as Λ CDM with spatial curvature, flat w CDM and flat w_0w_a CDM. Since $DM_{\text{IGM}} \propto \Omega_b H_0$, we find $\Omega_b h^2$ and H_0 are degenerate, and unconstrained by FRBs observations alone. And as a result, the other cosmological parameters are very weakly constrained, if at all. In all models considered here, the measurement precision on Ω_m is a few tens of percent, when using the most optimistic catalogue with no priors. This is an order of magnitude larger than current constraints coming from CBSH. To determine whether FRBs will improve current constraints, we have included in our FRB analysis realistic priors in the form of the CBSH covariance matrix. With this we showed that $\Omega_b h^2$ and Ω_k are the only two parameters that are better constrained when FRBs are included. All dark energy equation of state parameters are poorly constrained by FRBs.

To investigate how sample size and IGM inhomogeneity affect the resulting constraints, we constructed a number of mock catalogues while varying N_{FRB} and σ_{IGM} . We find that the inhomogeneity of the IGM poses a serious challenge to the ability of FRBs to improve current constraints. For all model parameterisations that we have considered here, we find that only the most optimistic FRB catalogue gives any appreciable improvement in the current CBSH constraints. For this catalogue we assumed a relatively low DM variance due to the IGM, with $\sigma_{\text{IGM}} = 200 \text{ pccm}^{-3}$, and a large number of events, with $N_{\text{FRB}} = 1000$. Crucially, these events require followup observations to acquire redshift information, which would require ~ 100 days of dedicated optical spectroscopic follow-up. Increasing the IGM inhomogeneity to $\sigma_{\text{IGM}} = 400 \text{ pccm}^{-3}$, or decreasing the sample size to $N_{\text{FRB}} = 100$ causes the resulting constraints to be dominated by their priors.

Future 21cm IM experiments designed to measure the BAO wiggles in the matter power spectrum will pro-

vide independent constraints on cosmological parameters at low/intermediate redshifts. While these observations do not constrain Ω_b , they will provide competitive constraints on H_0 and Ω_m (within the Λ CDM model). Since these experiments are expected to detect many FRBs during the course of their observations, we have investigated combining the BAO constraints with FRB data. We find that this produces a constraint on $\Omega_b h^2$ comparable to the existing one coming from CBSH observations. Thus, this approach may provide a novel low/intermediate redshift probe of the cosmic baryon density, independent of high redshift CMB data.

The biggest promise of FRB observations seems to be in locating the missing baryons, and not testing concordance or measuring the dark energy equation of state. This may change should one be able to mitigate the effect of IGM variance and the DM contribution from the host galaxy. There are however some caveats. We have assumed that f_{IGM} is not evolving with time, and its value is known perfectly. We have assumed perfect knowledge of DM_{MW} , and that it can be reliably subtracted from DM_{obs} , which is not practical as is known from pulsar observations. Also, we have assumed no error in the redshift of the FRBs. Including these additional sources of uncertainty will weaken any constraints we have obtained here.

We thank Jonathan Sievers and Kavilan Moodley for helpful comments. A. Walters is funded by a grantholder bursary from the National Research Foundation of South Africa (NRF) Competitive Programme for Rated Researchers (Grant Number 91552). A. Weltman gratefully acknowledges financial support from the Department of Science and Technology and South African Research Chairs Initiative of the NRF. The Dunlap Institute is funded through an endowment established by the David Dunlap family and the University of Toronto. B.M.G. acknowledges the support of the Natural Sciences and Engineering Research Council of Canada (NSERC) through grant RGPIN-2015-05948, and of the Canada Research Chairs program. Y.Z.M. acknowledges the support by NRF (no. 105925). A. Witzemann acknowledges support from the South African Square Kilometre Array Project and NRF. Any opinion, finding and conclusion or recommendation expressed in this material is that of the authors and the NRF does not accept any liability in this regard.

REFERENCES

- Abbott, B. P., Abbott, R., Abbott, T. D., et al. 2017, *Nature*, 551, 85
- Anderson, L., Aubourg, É., Bailey, S., et al. 2014, *MNRAS*, 441, 24

- Bandura, K., Addison, G. E., Amiri, M., et al. 2014, in *Proc. SPIE*, Vol. 9145, Ground-based and Airborne Telescopes V, 914522
- Becker, G. D., Bolton, J. S., Haehnelt, M. G., & Sargent, W. L. W. 2011, *MNRAS*, 410, 1096
- Beloborodov, A. M. 2017, *ApJL*, 843, L26
- Betoule, M., Kessler, R., Guy, J., et al. 2014, *A&A*, 568, A22
- Beutler, F., Blake, C., Colless, M., et al. 2011, *MNRAS*, 416, 3017
- Bull, P., Ferreira, P. G., Patel, P., & Santos, M. G. 2015, *ApJ*, 803, 21
- Burke-Spolaor, S., & Bannister, K. W. 2014, *ApJ*, 792, 19
- Caleb, M., Flynn, C., Bailes, M., et al. 2017, *MNRAS*, 468, 3746
- Champion, D. J., Petroff, E., Kramer, M., et al. 2016, *MNRAS*, 460, L30
- Chevallier, M., & Polarski, D. 2001, *International Journal of Modern Physics D*, 10, 213
- Cooke, R. J., Pettini, M., Nollett, K. M., & Jorgenson, R. 2016, *ApJ*, 830, 148
- Cordes, J. M., & Wasserman, I. 2016, *MNRAS*, 457, 232
- Deng, W., & Zhang, B. 2014, *ApJL*, 783, L35
- DES Collaboration, Abbott, T. M. C., Abdalla, F. B., et al. 2017, *ArXiv e-prints*, arXiv:1708.01530
- Dvorkin, I., Vangioni, E., Silk, J., Petitjean, P., & Olive, K. A. 2016, *MNRAS*, 458, L104
- Fialkov, A., & Loeb, A. 2017, *ApJL*, 846, L27
- Foreman-Mackey, D., Hogg, D. W., Lang, D., & Goodman, J. 2013, *PASP*, 125, 306
- Fuller, J., & Ott, C. D. 2015, *MNRAS*, 450, L71
- Gao, H., Li, Z., & Zhang, B. 2014, *ApJ*, 788, 189
- Ghisellini, G. 2017, *MNRAS*, 465, L30
- Ghisellini, G., & Locatelli, N. 2017, *ArXiv e-prints*, arXiv:1708.07507
- Gu, W.-M., Dong, Y.-Z., Liu, T., Ma, R., & Wang, J. 2016, *ApJL*, 823, L28
- Hinshaw, G., Larson, D., Komatsu, E., et al. 2013, *ApJS*, 208, 19
- Huterer, D., & Shafer, D. L. 2017, *ArXiv e-prints*, arXiv:1709.01091
- Joyce, A., Jain, B., Khoury, J., & Trodden, M. 2015, *PhR*, 568, 1
- Kashiyama, K., Ioka, K., & Mészáros, P. 2013, *ApJL*, 776, L39
- Katz, J. I. 2017, *MNRAS*, 469, L39
- Keane, E. F., Kramer, M., Lyne, A. G., Stappers, B. W., & McLaughlin, M. A. 2011, *MNRAS*, 415, 3065
- Keane, E. F., Johnston, S., Bhandari, S., et al. 2016, *Nature*, 530, 453
- Kowalski, M., Rubin, D., Aldering, G., et al. 2008, *ApJ*, 686, 749
- Kumar, P., Lu, W., & Bhattacharya, M. 2017, *MNRAS*, 468, 2726
- Li, M., Li, X.-D., Wang, S., & Wang, Y. 2011, *Commun. Theor. Phys.*, 56, 525
- Linder, E. V. 2003, *Physical Review Letters*, 90, 091301
- Locatelli, N., & Ghibellini, G. 2017, *ArXiv e-prints*, arXiv:1708.06352
- Lorimer, D. R., Bailes, M., McLaughlin, M. A., Narkevic, D. J., & Crawford, F. 2007, *Science*, 318, 777
- Lyubarsky, Y. 2014, *MNRAS*, 442, L9
- Masui, K., Lin, H.-H., Sievers, J., et al. 2015, *Nature*, 528, 523
- McQuinn, M. 2014, *ApJL*, 780, L33
- Meiksin, A. A. 2009, *Reviews of Modern Physics*, 81, 1405
- Newburgh, L. B., Bandura, K., Bucher, M. A., et al. 2016, in *Proc. SPIE*, Vol. 9906, Ground-based and Airborne Telescopes VI, 99065X
- Petroff, E., Bailes, M., Barr, E. D., et al. 2015, *MNRAS*, 447, 246
- Petroff, E., Barr, E. D., Jameson, A., et al. 2016, *PASA*, 33, e045
- Petroff, E., Burke-Spolaor, S., Keane, E. F., et al. 2017, *MNRAS*, 469, 4465
- Planck Collaboration, Ade, P. A. R., Aghanim, N., et al. 2016a, *A&A*, 594, A13
- . 2016b, *A&A*, 594, A14
- Rajwade, K. M., & Lorimer, D. R. 2017, *MNRAS*, 465, 2286
- Räsänen, S., Bolejko, K., & Finoguenov, A. 2015, *Physical Review Letters*, 115, 101301
- Ravi, V., Shannon, R. M., & Jameson, A. 2015, *ApJL*, 799, L5
- Ravi, V., Shannon, R. M., Bailes, M., et al. 2016, *Science*, 354, 1249
- Riess, A. G., Strolger, L.-G., Tonry, J., et al. 2004, *ApJ*, 607, 665
- Riess, A. G., Strolger, L.-G., Casertano, S., et al. 2007, *ApJ*, 659, 98
- Riess, A. G., Macri, L. M., Hoffmann, S. L., et al. 2016, *ApJ*, 826, 56
- Ross, A. J., Samushia, L., Howlett, C., et al. 2015, *MNRAS*, 449, 835
- Shull, J. M., Smith, B. D., & Danforth, C. W. 2012, *ApJ*, 759, 23
- Smith, R. E., Peacock, J. A., Jenkins, A., et al. 2003, *MNRAS*, 341, 1311
- Spitler, L. G., Cordes, J. M., Hessels, J. W. T., et al. 2014, *ApJ*, 790, 101

- Tendulkar, S. P., Bassa, C. G., Cordes, J. M., et al. 2017, ApJL, 834, L7
- Thompson, C. 2017, ApJ, 844, 162
- Thornton, D., Stappers, B., Bailes, M., et al. 2013, Science, 341, 53
- Totani, T. 2013, PASJ, 65, L12
- Wang, J.-S., Yang, Y.-P., Wu, X.-F., Dai, Z.-G., & Wang, F.-Y. 2016, ApJL, 822, L7
- Witzemann, A., Bull, P., Clarkson, C., et al. 2017, ArXiv e-prints, arXiv:1711.02179
- Xu, J., & Han, J. L. 2015, Research in Astronomy and Astrophysics, 15, 1629
- Yang, Y.-P., & Zhang, B. 2016, ApJL, 830, L31
- Yao, J. M., Manchester, R. N., & Wang, N. 2017, Astrophys. J., 835, 29
- Zhang, B. 2014, ApJL, 780, L21
- Zhou, B., Li, X., Wang, T., Fan, Y.-Z., & Wei, D.-M. 2014, PhRvD, 89, 107303